NANO LETTERS

2007
Vol. 7, No. 8
2341−2345

Direct Observation of Surface Mode Excitation and Slow Light Coupling in Photonic Crystal Waveguides

Valentyn S. Volkov,*,† Sergey I. Bozhevolnyi,† Lars H. Frandsen,‡ and Martin Kristensen§

Department of Physics and Nanotechnology, Aalborg University, Skjernvej 4A, DK-9220 Aalborg Øst, Denmark, COM•DTU, Department of Communications, Optics & Materials, Nano•DTU, Technical University of Denmark, DK-2800 Kgs Lyngby, Denmark, and Department of Physics and Astronomy and Interdisciplinary Nanoscience Center (iNANO), University of Aarhus, Ny Munkegade, Building 1520, DK-8000 Aarhus C, Denmark

Received April 26, 2007; Revised Manuscript Received June 10, 2007

ABSTRACT

A scanning near-field optical microscope (SNOM) is used to systematically study the properties of guided modes in linear and slow-light regimes of silicon-on-insulator (SOI)-based photonic crystal waveguides (PhCWs) with different terminations of the photonic lattice. High quality SNOM images are obtained for light at telecom wavelengths propagating in the PhCW, demonstrating *directly*, for the first time to our knowledge, drastic widening of the PhCW guided mode in the slow-light regime and excitation of surface waves at the PhCW interface along with their feeding into the guided mode for the lattice terminations corresponding to significantly reduced coupling loss.

Nanostructured materials with sufficiently strong periodic modulation of the refractive index behave toward light as semiconductors do toward electrons, forbidding the propagation of light within a range of frequencies residing in the so-called photonic band gap (PBG).[1] The PBG materials, also called photonic crystals (PhCs), possess many interesting physical properties. For instance, by introducing point and/or line defects in PhCs, light can be localized[2] in and guided[3] along the defects, opening a way to the realization of highly integrated optical circuits. The research within PhC waveguides (PhCWs) has now matured to a level where present fabrication technologies allow the fabrication of PhCWs with sufficient low insertion losses.[4] The main focus is currently put upon exploring unique PhCW properties for the realization of photonic functionalities that are unattainable within conventional integrated optics. One important development is related to the possibility of significantly slowing down the propagation of light in PhCWs, and group velocities several hundreds times lower than the speed of light in vacuum have recently been reported by several groups.[5−8] However, before the slow-light phenomenon may be exploited for practical applications (e.g., for compact delay lines and all-optical storage devices), one should first deal with the problem of increasingly large impedance mismatch between the access ridge waveguide and (slow-light) PhCW modes due to an increase of the group index in the slow-light regime that prevents efficient coupling into (and out of) the PhCW. Recent investigations have shown both theoretically[9−11] and experimentally[12] that the coupling of light into/out of a PhCW can be noticeably enhanced by creating a specific periodic modulation (termination) of the crystal lattice surrounding the entrance/outlet of the PhCW. This enhanced coupling is related to the excitation of electromagnetic surface modes propagating along and localized at the PhC interface having the appropriate lattice termination.[9] Meade et al.[13] were the first to study and discuss theoretically the surface states of truncated PhCs, but their existence has not yet been revealed experimentally, probably because of their indirect evanescent nature. However, they have been indirectly deduced from transmission measurements showing the dependence of the coupling efficiency on the group index for different terminations of the PhC lattice[12] and the influence of surface termination on the dispersion of surface states.[14]

In this letter, we report what we believe to be the first *direct* observations of PhCW excitation in the slow-light regime using a scanning near-field optical microscope (SNOM), *visualizing* surface waves at the PhCW interface

* To whom correspondence should be addressed. E-mail: volkov@physics.aau.dk.
† Aalborg University.
‡ Technical University of Denmark.
§ University of Aarhus.

10.1021/nl0709928 CCC: $37.00
Published on Web 07/07/2007

along with their feeding into the guided mode for the lattice terminations corresponding to significantly reduced coupling loss. SNOM imaging has previously been used to study the angular spread of directional beams emerging from two-dimensional (2D) PhCWs[15] and light propagation at telecom wavelengths (mainly for the linear regime) along straight and bent regions of silicon-on-insulator (SOI) PhCWs[16−19] as well as for phase-sensitive and time-resolved visualization of pulse propagation in PhCWs.[7,20] However, the potential of the SNOM technique to map the optical field intensity distributions in PhCWs operating in the slow-light regime has not yet been fully exploited.

The experimental setup consists of a collection SNOM with a tapered aluminum (Al)-coated fiber (aperture diameter $\approx$ 150 nm) used as a probe and an arrangement for launching tunable (1430−1620 nm) transverse electric (TE)-polarized (the electric field is parallel to the sample surface plane) radiation into the input ridge waveguide by careful positioning of a tapered-lensed polarization-maintaining single-mode fiber. The adjustment of the in-coupling fiber with respect to the sample facet was accomplished by monitoring the light propagation along the sample surface with the help of a far-field microscopic arrangement.[16] Following the fiber adjustment, the intensity distribution near the sample surface was probed with the Al-coated sharp fiber tip of the SNOM. The tip can be scanned along the sample surface at a constant distance of a few nanometers maintained by shear-force feedback. Near-field radiation scattered by the tip is partially collected by the fiber itself and propagates in the form of fiber modes toward the other end of the fiber, where it is detected by a femtowatt InGaAs photoreceiver. The PhCWs were fabricated in the top silicon layer of a SOI wafer. The photonic crystal lattice with pitch $\Lambda \approx 400$ nm penetrates the top 338 nm silicon slab placed on a 1 μm thick buffer layer of silica. The photonic crystal patterns were defined by using electron-beam lithography and transferred to the silicon by inductively coupled plasma reactive ions etching.[21] Holes were arranged in a triangular array (hole diameter $\approx$ 275 nm), and a single row of missing holes defined the PhCWs along the ΓK direction of the irreducible Brillioin zone of the lattice.[1] Using a similar PhCW, we have previously observed the transition to the slow-light waveguiding regime (with the group velocity slowing down to $\sim c/30$, with c being the speed of light in vacuum) when increasing the light wavelength up to the band gap edge.[17]

A scanning electron microscopy (SEM) image of a typical fabricated PhCW is shown in Figure 1a. The sample contained a central PhC area connected to tapered access ridge waveguides that are gradually tapered from a width of $\sim$4 μm at the sample facet to $\sim$700 nm at the PhC interface and used to route the light into and out of the PhCWs. To investigate the influence of surface termination, a set of PhCW structures was fabricated in which the truncation of the PhCWs at the ridge−PhC interface was varied by changing the termination parameter from $\tau \approx 0.36$ to $\tau \approx 0.75$ as schematically shown in Figure 1b. The fabricated PhCWs have been excited at different telecom wavelengths (for TE-polarized light) and imaged with the SNOM. The

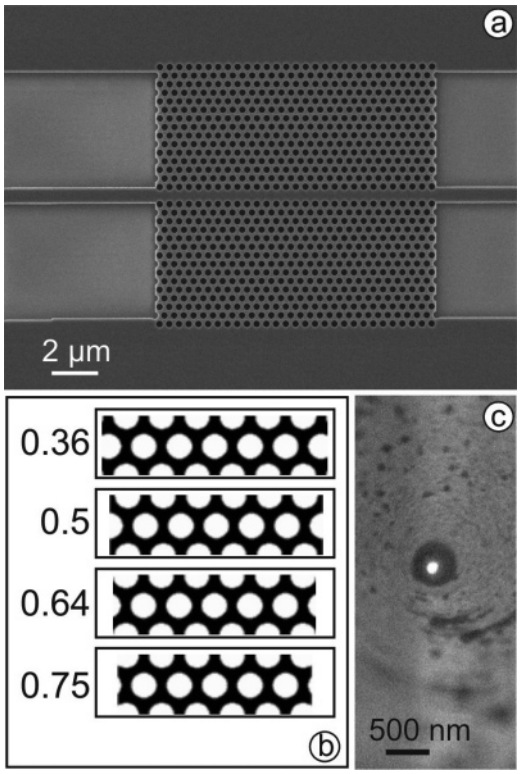

Figure 1. (a) Scanning electron micrograph of the PhCW with the termination of the ridge−PhC interface ($\tau \approx 0.5$). (b) Schematic representation of the truncated lattices of the PhC structure for different interface terminations. (c) SEM image of the Al-coated fiber tip used in the experiment.

topographical and near-field optical images obtained for the PhCW with $\tau \approx 0.75$ in the broad wavelength range (1430−1551 nm) are shown in Figure 2. On the topographical image in Figure 2a, one can easily recognize the pattern of holes that forms the PhCW. The near-field optical images in Figure 2b−h for different wavelengths exhibit several features appearing also on the images obtained for other waveguides with different terminations. For instance, we found that in the wavelength range 1430−1520 nm (corresponding to the linear regime of the PhCW) the recorded intensity distributions are well confined to the line of missing holes (defining the PhCW) exhibiting wavelength-dependent intensity variations along the propagation direction. In general, the cross sections (perpendicular to the propagation direction) of intensity distributions varied gradually with the increase of the wavelength, redistributing the light power across the PhCW area. In particular, we have observed the expansion of fields into the surrounding photonic crystal environment when approaching the cutoff wavelength (for this PhCW located at 1551 nm): at short wavelengths (1430−1520 nm), the propagating mode is mostly confined within the line defect (Figure 2b−d) with the mode being close to the Gaussian distribution in shape, while in the wavelength range of 1530−1551 nm the mode field progressively spreads into the neighboring lines of holes forming the tridentlike transverse distribution (Figure 2e−h). The cross sections (not shown here) of these images made at the intensity maxima by averaging over a few lines through the PhCW showed the full width at half-maximum (FWHM) of the PhCW mode

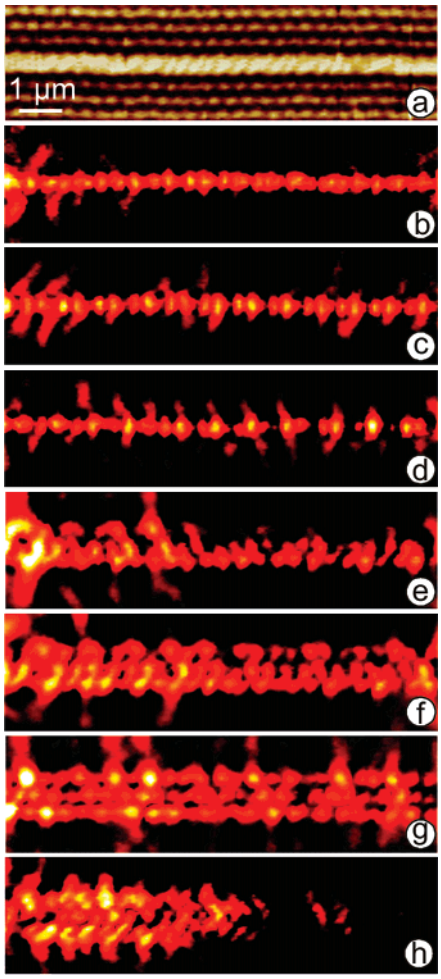

Figure 2. Pseudo-color (a) topographical and (b−h) near-field optical images ($10 \times 2.75\ \mu m^2$) obtained for the investigated PhCW with $\tau \approx 0.75$ at $\lambda \cong$ (b) 1430, (c) 1460, (d) 1500, (e) 1540, (f) 1547, (g) 1550, and (h) 1551 nm. SNOM images are oriented in a way so that the light propagates rightward in the horizontal direction.

to be close to ∼420 nm for the linear regime (at short wavelengths) and ∼1.2 μm for the slow-light regime (near the cutoff wavelength). The observed behavior of the PhCW slow-light mode is in agreement with the results of recently reported theoretical findings[22] where the modal field distributions for the fundamental even PBG mode for different wave vectors corresponding to linear and slow-light regimes have been presented.

The next step was to conduct SNOM imaging of all fabricated PhCW structures while paying attention to the possibility of exciting surface waves at the ridge−PhCW interface in the slow-light regime (Figure 3). The SNOM images obtained at short wavelengths are found to be rather similar for all investigated structures (compare Figure 3b and e). Light propagating in the input ridge waveguides, further along the PhCWs, and into the output waveguides is clearly seen, as well as the light scattering at the junctions between the PhC and ridge waveguides. We observed drastic changes in the field intensity distributions when approaching the cutoff wavelength for different PhCWs. Together with the aforementioned spreading of the PhCW mode (observed for

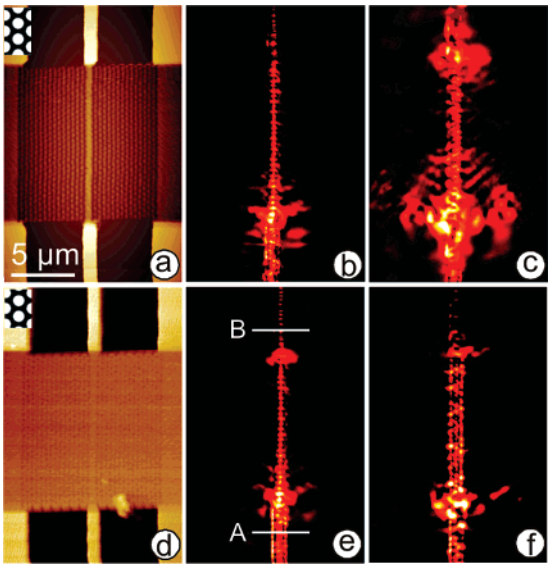

Figure 3. Pseudo-color (a and d) topographical and (b, c, e, and f) near-field optical images ($14 \times 21\ \mu m^2$) obtained for the investigated PhCWs with different terminations (shown schematically in insets): (a) $\tau \approx 0.5$ and (d) $\tau \approx 0.75$ at $\lambda \cong$ (b and e) 1430 and (c and f) 1545 nm, correspondingly. SNOM images are oriented in a way so that the light propagates upward in the vertical direction.

all PhCWs), the SNOM images obtained for the PhCW with $\tau \approx 0.5$ clearly showed excitation of surface waves (seen as the light spreading along the input PhC facet) in the wavelength range of 1535−1548 nm, with the best SNOM image being recorded at 1545 nm (Figure 3c). To facilitate the comparative analysis of this intriguing phenomenon, the SNOM images recorded in the linear and slow-light regimes were directly superimposed on the corresponding SEM images (Figure 4) by making use of the SNOM topographical images taken simultaneously with the optical ones (Figure 3). In this way, the excitation of surface waves in the slow-light regime (at the input ridge−PhC interface with $\tau \approx 0.5$) is clearly seen along with their *feeding* into the PhCW guided mode resulting in a triangle-like shape of the optical signal distribution (Figure 4b). This feeding represents, in our opinion, the main physical mechanism responsible for the enhanced coupling (in the slow-light regime) found previously for specific lattice terminations.[9−12] At the same time, it should be noted that we did not observe any evidence of surface waves for the PhCWs with other surface terminations [$\tau \approx 0.75$ (Figure 3f) or $\tau \approx 0.36$ and 0.64 (not shown here)].

The interest in surface wave excitation in PhCW structures has been primarily driven by the possibility of enhancing the efficiency of coupling into the slow-light PhCW mode.[12] To correlate the phenomena of surface wave excitation and enhanced coupling, we have further evaluated the transmission spectra (the corresponding output-to-input ratio as a function of the light wavelength) for the investigated PhCWs (Figure 5) by making the optical image average cross sections perpendicular to the propagation direction before and after the PhCs (along the lines schematically shown in Figure 3e). It is seen that the transmission spectra for PhCWs with terminations $\tau \approx 0.36$, 0.5, 0.64, and 0.75 are rather similar for most of the wavelengths. The notable differences in the

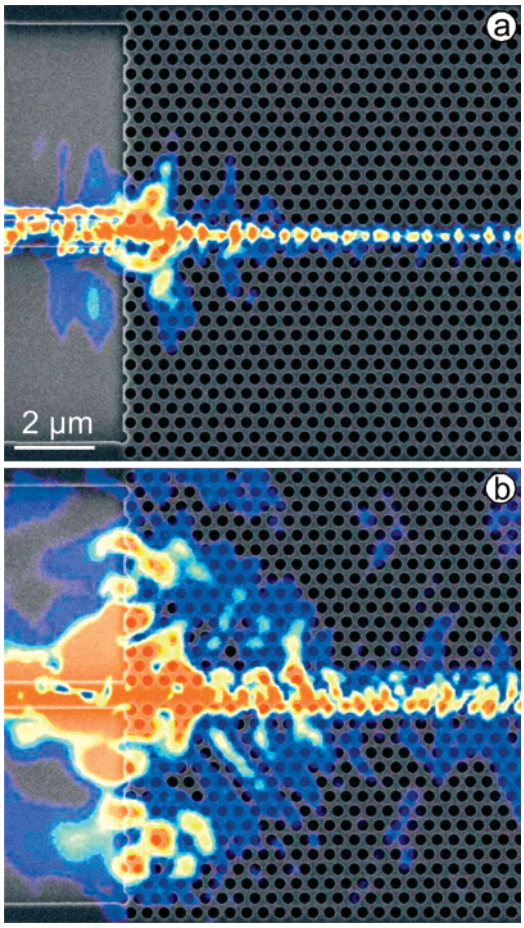

Figure 4. Pseudo-color near-field optical images recorded in the (a) linear (at $\lambda \cong 1430$ nm) and (b) slow-light (at $\lambda \cong 1545$ nm) regimes and directly superimposed on the corresponding SEM images by making use of the corresponding SNOM topographical images taken simultaneously with the optical ones (Figure 3). Images are oriented in a way so that the light propagates rightward in the horizontal direction.

spectra are observed at wavelengths longer than ~1530 nm and closer to the cutoff at 1551 nm. This wavelength range corresponds to the long-wavelength band gap edge characterized with increasingly slow group velocities, for example, observed previously with similar samples.[17] More specifically, in the wavelength range of 1535−1548 nm, the transmission spectrum obtained for the PhCW with the termination $\tau \approx 0.5$ demonstrates a pronounced increase in transmission (i.e., enhanced coupling) with the maximum centered at 1545 nm, corresponding precisely to the most pronounced excitation of surface waves (Figure 4b). In the same wavelength range, the transmission for PhCWs with other terminations ($\tau \approx 0.36$, 0.64, and 0.75) was found to gradually and monotonically decrease (Figure 5). This circumstance, most probably, indicates that for these waveguide terminations surface waves do not exist or/and they are not in resonance with slow-light PhCW modes and cannot be efficiently detected with our SNOM.

In conclusion, using the collection SNOM, we have experimentally investigated the properties of guided modes in PhCWs with different terminations of the ridge−PhC interface in the linear and slow-light regimes. High quality

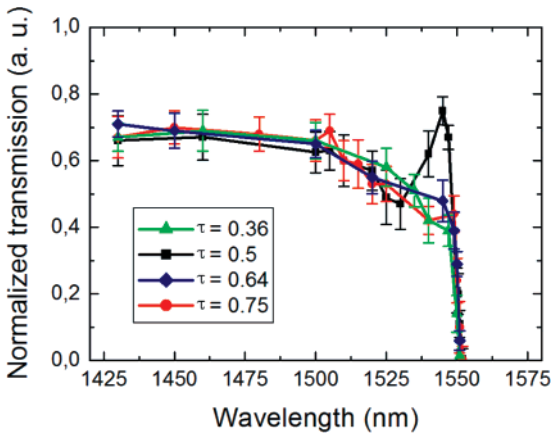

Figure 5. Experimental transmission spectra obtained for PhCWs with different terminations of the ridge−PhC interface. The output-to-input ratios were obtained by using average (along 8 lines) cross sections of near-field optical images (similar to that shown in Figure 3) taken before and after PhCWs along the lines marked with A and B (see Figure 3e) for both (input and output) ridge waveguides. The error bars are estimated from the maximum variation in the ratio when placing the averaging windows at different positions along the input and output slab waveguides.

SNOM images of these waveguides excited at telecom wavelengths have been obtained and used to characterize the PBG structures studied. It was found that the near-field distributions of mode profiles show significant spreading of the fields out of the PhC waveguides when approaching the cutoff wavelength. These experimental results are found to be in a good agreement with theoretical results reported recently.[22] Finally, the existence of surface waves at the ridge−PhC interface has been for the first time directly demonstrated for the PhCW with the termination $\tau \approx 0.5$, and their influence on slow-light coupling has been analyzed and found to be playing a significant role in reducing coupling loss.

Acknowledgment. This research is carried out in the framework of the national frame programme "Planar Integrated Photonic Band Gap Elements (PIPE)" supported by the Danish Technical Research Council, Contract No. 26-03-0158.

References

(1) Joannopoulos, J. D.; Meade, R. D.; Winn, J. N. *Photonic Crystals: Molding the Flow of Light*; Princeton University Press: Princeton, NJ, 1995.
(2) Yoshie, T.; Vučković, J.; Scherer, A.; Chen, H.; Deppe, D. *Appl. Phys. Lett.* **2001**, *79*, 4289.
(3) Lončar, M.; Doll, T.; Vučković, J.; Scherer, A. *J. Lightwave Technol.* **2000**, *18*, 1402.
(4) McNab, S. J.; Moll, N.; Vlasov, Y. A. *Opt. Express* **2003**, *11*, 2927.
(5) Notomi, M.; Yamada, K.; Shinya, A.; Takahashi, J.; Takahashi, C.; Yokohama, I. *Phys. Rev. Lett.* **2001**, *87*, 253902.
(6) Vlasov, Y. A.; O'Boyle, M.; Hamann, H. F.; McNab, S. J. *Nature* **2005**, *438*, 65.
(7) Gersen, H.; Karle, T. J.; Engelen, R. J. P.; Bogaerts, W.; Korterik, J. P.; van Hulst, N. F.; Krauss, T. F.; Kuipers, L. *Phys. Rev. Lett.* **2005**, *94*, 073903.
(8) Jacobsen, R. S.; Lavrinenko, A. V.; Frandsen, L. H.; Peucheret, C.; Zsigri, B.; Moulin, G.; Fage-Pedersen, J.; Borel, P. I. *Opt. Express* **2005**, *13*, 7861.
(9) Moreno, E.; García-Vidal, F. J.; Martín-Moreno, L. *Phys. Rev. B* **2004**, *69*, 121402.

(10) Moreno, E.; Martín-Moreno, L.; García-Vidal, F. J. *Photonics Nanostruct.: Fundam. Appl.* **2004**, *2*, 97.
(11) Zhu, Z.-H.; Ye, W.-M.; Ji, J.-R.; Yuan, X.-D.; Zen, C. *Appl. Phys. B* **2007**, *86*, 327.
(12) Vlasov, Y. A.; McNab, S. J. *Opt. Lett.* **2006**, *31*, 65.
(13) Meade, R. D.; Brommer, K D.; Rappe, A. M.; Joannopoulos, J. D. *Phys. Rev. B* **1991**, *44*, 10961.
(14) Vlasov, Y. A.; Moll, N.; McNab, S. J. *Opt. Lett.* **2004**, *29*, 2175.
(15) Kramper, P.; Agio, M.; Soukoulis, C. M.; Birner, A.; Müller, F.; Wehrspohn, R. B.; Gösele, U.; Sandoghdar, V. *Phys. Rev. Lett.* **2004**, *92*, 113903.
(16) Bozhevolnyi, S. I.; Volkov, V. S. *Phil. Trans. R. Soc. London, Ser. A* **2004**, *362*, 757.
(17) Volkov, V. S.; Bozhevolnyi, S. I.; Borel, P. I.; Frandsen, L. H.; Kristensen, M. *Phys. Rev. B* **2005**, *72*, 035118.
(18) Abashin, M.; Tortora, P.; Märki, I.; Levy, U.; Nakagawa, W.; Vaccaro, L.; Herzig, H. P.; Fainman, Y. *Opt. Express* **2006**, *14*, 1643.
(19) Tao, H.-H.; Liu, R.-J.; Li, Z.-Y.; Feng, S.; Liu, Y.-Z.; Ren, C.; Cheng, B.-Y.; Zhang, D.-Z.; Ma, H.-Q.; Wu, L.-A.; Zhang, Z.-B. *Phys. Rev. B* **2006**, *74*, 205111.
(20) Gersen, H.; Karle, T. J.; Engelen, R. J. P.; Bogaerts, W.; Korterik, J. P.; van Hulst, N. F.; Krauss, T. F.; Kuipers, L. *Phys. Rev. Lett.* **2005**, *94*, 123901.
(21) Borel, P. I.; Frandsen, L. H.; Thorhauge, M.; Harpøth, A.; Zhuang, Y. X.; Kristensen, M. *Opt. Express* **2003**, *11*, 1757.
(22) Frandsen, L. H.; Lavrinenko, A. V.; Fage-Pedersen, J.; Borel, P. I. *Opt. Express* **2006**, *14*, 9444.

NL0709928